# Investigation of dependence of gas flow on the geometry of cyclonic seperators by CFD simulation

Michael Harasek, Andras Horvath, Christian Jordan

Institute of Chemical Engineering, Vienna University of Technology
Getreidemarkt 9/166, 1060 Vienna, Austria
Phone: +43 1 58801 159 25, Fax: +43 1 58801 159 99
email: mharasek@mail.zserv.tuwien.ac.at

**Abstract** Several types of flow structures in cyclones were found in recent publications. The published propositions of the internal flow structure were partly derived from measurements, partly from simulations and in some cases both simulations and measurements were carried out. As a means for structuring the findings the publications were split into two arbitrary classes. Each class represented a certain feature of the axial velocity profile of the gas flow inside the cyclone. Class $V$ represents cyclones with a maximum of the axial velocity at the vortex core of the cyclone, whereas Class $W$ represents cyclones with an axial velocity profile that resembles an upside down W. This class has a local minimum of axial velocity at the vortex core or even displays backflow. The geometries of the cyclones belonging either to Class V or to Class W showed only small relative differences. It was assumed that the diameter of the vortex finder had a great influence on the class membership. This influence could be simulated reproduceably for different basic geometries.

Laser Doppler Anemometry (LDA) experiments were carried out on a laboratory scale cyclone to verify simulation results. The results of cyclones which were investigated in previously published papers were used as a basis for developing a method of simulation to validate numerical results and class membership.

## Contents

## 1 Introduction

In publications regarding Computational Fluid Dynamics (CFD) of gas flow in cylonic seperators several types of flow structures were found. The published propositions of the internal flow structure were partly derived from measurements, partly from simulations and in some cases both simulations and measurements were carried out (see Table 1).

As a means for structuring the findings the published flow structures were split into two classes called V and W (see Fig. 1). Each class represented a certain feature of the axial velocity profile of the gas flow inside the cyclone. The axial profiles were chosen because they showed the greatest relative differences between similar cases (defined by geometry and flow rate). The other velocity profiles (tangential velocity, absolute velocity) were rather comparable for similar cases. *Class V* represents cyclones with a maximum of the axial velocity at the vortex core of the cyclone, whereas *Class W* represents cyclones with an axial velocity profile that resembles an upside down W. This class has a minimum of axial velocity at the vortex core or even displays backflow. In contrary to Class V the maximum of axial velocity in Class W is approximately at the position of the vortex finder radius.

The geometries of the cyclones belonging either to Class V or to Class W showed only small relative differences of dimensionless length-parameters. It was assumed that the relative diameter of the vortex finder had a great influence on the class membership. As one shall see the effect of this influence could be simulated reproduceably for different basic geometries and derivates thereof.

First computational efforts in the field of flow simulation of cyclones were done by Boysan et al. (1982) utilising 2D-axisymmetric assumptions which do not necessarily apply to typical cyclonic flows because the asymmetric inlet-boundary condition are not taken into account. Newer findings (see Hoekstra et al. (1999) and Gorton-Hülgerth (1998)) also propose a slowly precessing asymmetric vortex core (PVC). Computational power and data storage capabilities have incredibly increased since then allowing a far more detailed look at complex flows. In CFD high spatial resolution can be achieved easily, but detailed calculation results are not necessarily physically correct. Neither must a result with a low spatial resolution be physically wrong.

The first goal of this work was to develop a basic method for trustworthy simulation results (especially when considering new and challenging geometries) using the widely known geometry preprocessor GAMBIT™ (Version 2.0) in combination with the finite volume CFD code FLUENT™ (Version 6.0), which also serves as a postprocessor. The second goal was the correct prediction of class membership for different cyclone geometries and derivates thereof.

The correct prediction of the gas flow inside the cyclone is a necessity for predicting pressure drop and particle transport, which lies partly beyond the scope of this research work.

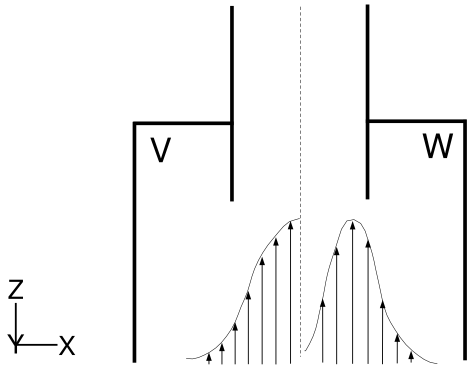


Figure 1: Schematic illustration of the the axial flow profile of the two classes of cyclones found in the literature mentioned in Table 1. This figure shows the upper cylindrical part of a cyclone, the vortex finder and the axis of symmetry.

| Class V | Class W |
|---|---|
| **Simulation**<br>Griffiths and Boysan (1995), Yoshida (1996)<br>Frank and Yu (1999), Ma et al. (2000)<br>Horvath (2002) | **Simulation**<br>Slack et al. (2000), Peng et al. (2001) |
| **Measurement**<br>Solero and Coghe (2002)<br>Kim and Lee (1990) | **Measurement**<br>Obermair (2002) |
| | **Simulation and Measurement**<br>Gorton-Hülgerth (1998)<br>Hoekstra et al. (1999)<br>Fredriksson (1999), Slack (2001) |

Table 1: Structured listing of considered cases.

# 2 Simulation

## 2.1 Validation of Simulation Method

To validate the simulation method three different representative geometries from the available literature were chosen (see Table 1 and Fig. 3). The simulation engine of FLUENT™ was mostly regarded as a black-box (from the process engineer's point of view). It is known from several publications[1] that the following modelling assumptions do not necessarily yield physically correct simulation results for cyclonic gas flow[2]:

- k-$\epsilon$ or RNG-k-$\epsilon$-turbulence-model
- tetrahedral grid in main flow regions
- 1$^{st}$ order discretisation schemes for flow governing variables[3]

It can easily be shown[4] that no Class W profile of axial velocity can be achieved if any of the above settings is passed to the simulation engine. The simulation results can nonetheless be physically correct if the cyclone belongs to Class V but that is usually unknown in advance. It was found that all of the following points had to be met to reproduce the simulation result for a class W cyclone:

- Hexahedral grid throughout the volume of the cyclone (except in dust collector)
- Higher order discretisation
- RSM (Reynolds Stress Model)

[1] Gorton-Hülgerth (1998), Hoekstra et al. (1999), Fredriksson (1999), Slack et al. (2000) and Anh (2004) among others.

[2] Most problematic to simulate is the region of the vortex core, which displays highly fluctuating velocity fields, backflow phenomena and generally speaking a transient behaviour. This is the region were different turbulence models (and also different grids) produce solutions deviating from each other to a high degree.

[3] see Fluent (2001) p. 5-11 ff.

[4] See comparison of measurements and simulation results in Fredriksson (1999) p. 90 ff., Hoekstra et al. (1999) p. 2064 and Anh (2004) p. 118 ff.

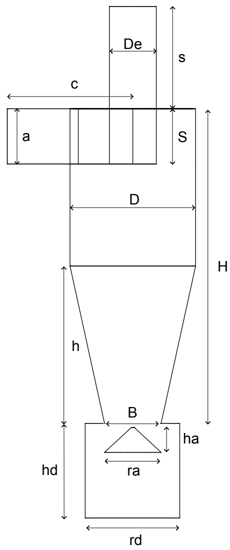


| | |
|---|---|
| D | Diameter of cyclone |
| De | Diameter of vortex-finder |
| S | Height of vortex-finder inside cyclone |
| s | Height of vortex-finder outside cyclone |
| h | Height of frustum section |
| H | Total height of cyclone (without dust collector) |
| a;b;c | Height, depth and width of tangential inlet |
| B | Diameter of aperture to dust collector |
| ha; ra | Height and radius of apex-cone |
| hd; rd | Height and radius of dust collector |

Figure 2: Description of geometry parameters

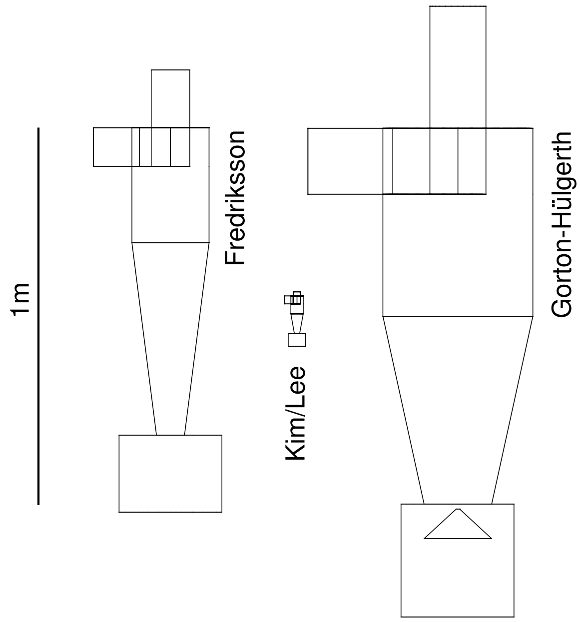


Figure 3: Outlines of successfully simulated geometries with reference scale (all designs have a tangential inlet and a centered vortex finder; the cyclone used by Gorton-Hülgerth has a built-in apex cone in the dust collector). The labels refer to the names of the authors (from left to right: Fredriksson (1999), Kim and Lee (1990), Gorton-Hülgerth (1998))

| | Fredriksson | Kim/Lee | Gorton-Hülgerth |
|---|---|---|---|
| Geometry | | | |
| D [m] | 0.2 | 0.0311 | 0.4 |
| De [m] | 0.1 | 0.08 | 0.15 |
| S [m] | 0.1 | 0.036 | 0.175 |
| s [m] | 0.15 | 0.016 | 0.325 |
| h [m] | 0.3 | 0.045 | 0.5 |
| H [m] | 0.8 | 0.095 | 1.0 |
| a; b; c [m] | 0.1; 0.04; 0.2 | 0.0143; 0.00629; 0.02 | 0.175; 0.1; 0.4 |
| B [m] | 0.072 | 0.013 | 0.18 |
| ha; ra [m] | – | – | 0.08; 0.09 |
| hd; rd [m] | 0.2; 0.133 | 0.0311; 0.02073 | 0.3; 0.15 |
| Air flow | | | |
| $\dot{V}$ $[m^3/s]$ | 0.08 | 0.0003066 | 0.222 |
| $v_x$ [m/s] | 20.0 | 3.4 | 12.7 |
| Simulation parameters | | | |
| Grid-type | hybrid | hybrid | hybrid |
| Number of cells | ≈ 645 000 | ≈ 56 000 | ≈ 478 000 |
| Turb. Model | RSM | Laminar/RSM | RSM |

Table 2: Geometry parameters, volumetric flow rate ($\dot{V}$), mean flow velocity at entry ($v_x$) and simulation parameters for the cases which were considered to validate the simulation method. $\varrho_{air} = 1.225\,kg/m^3$, $\nu_{air}$=1.4607·10$^{-5}$ $m^2$/s. Values for *Kim/Lee* were taken from their publication and are not rounded.

The geometries of the cyclones were constructed as depicted in Fig. 3 and the boundary conditions were assumed as follows:

- Inlet: plug flow (sufficient approximation of fully developed, turbulent pipe flow)
- Outlet: the "pressure outlet" setting in FLUENT™ is applied (no geometry downstream the vortex finder was simulated)

Both inlet and outlet turbulence intensities had to be estimated for boundary condition settings. As proposed in the FLUENT™-manual[5] the estimations were based on a formula for turbulence intensity in a fully developed duct

[5] Fluent (2001) p. 6-11 f.

flow.

$$I = 0.16 \cdot Re^{-\frac{1}{8}} \tag{1}$$

All of the calculations were done using the Reynolds Stress Model with standard parameters, non-equilibrium wall-functions and $2^{nd}$ order discretisation utilising a steady solver (time independent solution). Using these solver settings a good match with the published cases was achieved.

## 2.2 Grid generation

An important step in CFD is grid generation. A grid can either be structured, unstructured or block structured. It can be built of pyramidal, prismatic and/or exactly hexahedrally shaped cells. It is known that the structure of the grid has a great influence on the simulation result (see Anh (2004) p.119, Noriler et al. (2004)).

A detailed image of the surface grid for the geometry *Gorton-Hülgerth* De/D=0.375 viewed from the top of the cyclone can be seen in Fig. 4. The border of the vortex-finder is printed in bold linestyle. The grid inside the radius of the vortex-finder is unstructured. The grid outside the radius of the vortex finder is structured. A fully structured grid would yield a high gradient in cell volume near the symmetry-axis not suitable for simulations using RSM. The other cyclone geometries are meshed in a similar way by applying the *Cooper*-Scheme and projecting the surface grid at the cyclone top cover in z direction.

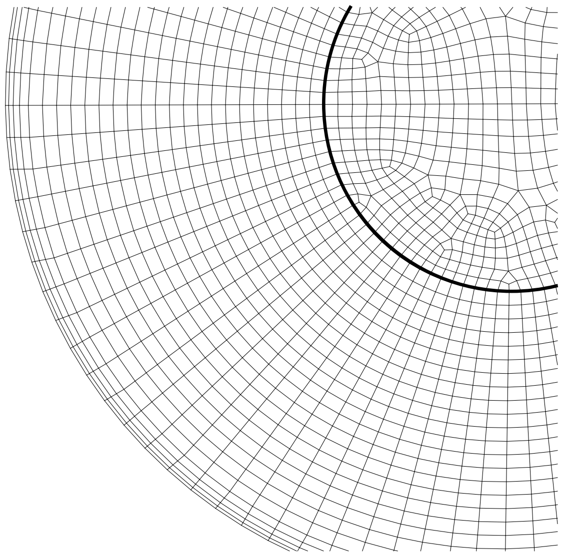

Figure 4: Detail of surface grid for geometry *Gorton-Hülgerth* De/D=0.375.

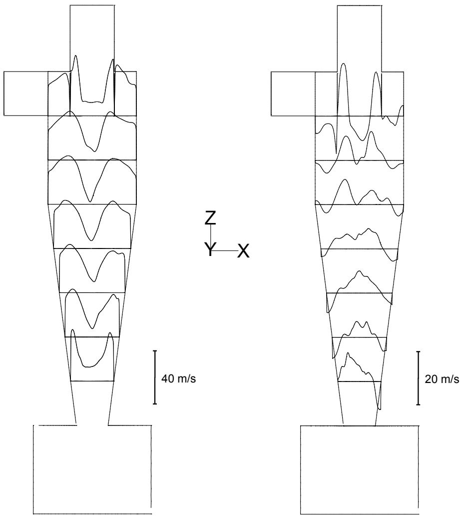


Figure 5: Simulation result for geometry *Fredriksson* De/D=0,5. Total number of cells: 645 000. Left: plot of absolute velocity [m/s], right: plot of axial velocity [m/s].

## 2.3 Geometry modification and results

Starting from the original geometries introduced in Fig. 3, modifications with vortex finder diameters larger and smaller than the validation-cases were constructed while keeping the other geometry parameters, the flow rate and the mesh structure constant. A small relative decrease of the dimensionless vortex-finder diameter De/D would change the simulation result from Class W to Class V. For the representative geometries *Fredriksson* and *Gorton-Hülgerth* the simulated results are depicted in Fig. 6, 7, 8 and 9. For all investigated geometries lower and upper De/D-values were found, where the simulation belongs to class V below the low value of De/D and to class W above the upper value of De/D (see Table 3). To prove this effect of the dimensionless vortex-finder diameter on the flow structure a laboratory-scale experiment was carried out.

| Geometry | De/D |
|---|---|
| Fredriksson | [0.4; 0.5] |
| Gorton-Hülgerth | [0.3; 0.375] |
| Kim-Lee | [0.26; 0.44] |

Table 3: Lower and upper values of De/D for simulation results belonging either to class V or to class W. Further investigations between the lower and upper boundary will be carried out.

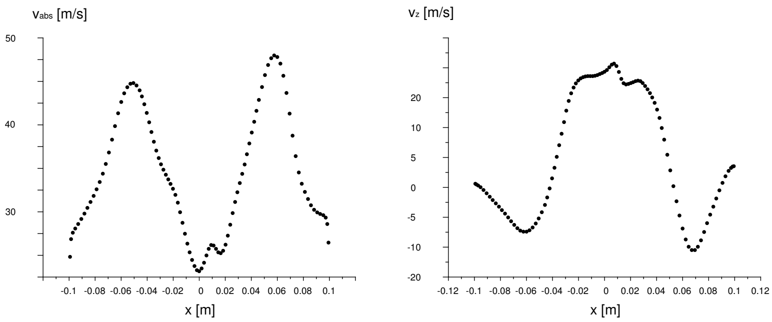


Figure 6: Example for **Class V**. Simulation result for Geometry *Fredriksson* De/D=0.4. Number of grid cells: 680 000. Velocity profile 0.1 m below vortex finder in xz-plane. Left: absolute velocity [m/s], right: axial velocity [m/s].

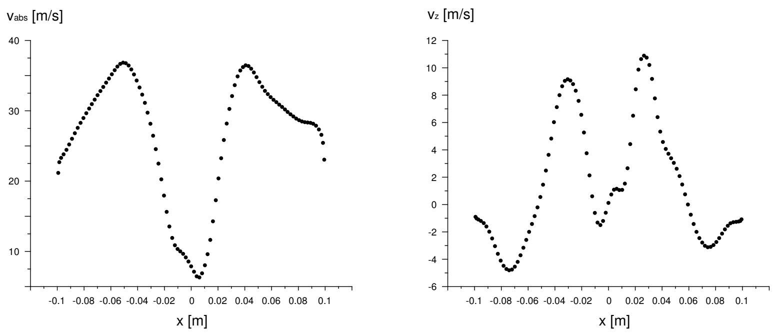


Figure 7: Example for **Class W**. Simulation result for Geometry *Fredriksson* De/D=0.5. Number of grid cells: 645 000. Velocity profile 0.1 m below vortex finder in xz-plane. Left: absolute velocity [m/s], right: axial velocity [m/s].

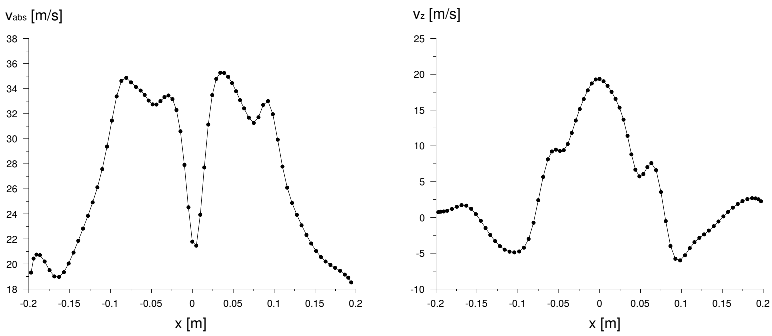


Figure 8: Example for **Class V**. Simulation result for Geometry *Gorton-Hülgerth* De/D=0.3. Number of grid cells: 465 000. Velocity profile 0.125 m below vortex finder in xz-plane. Left: absolute velocity [m/s], right: axial velocity [m/s].

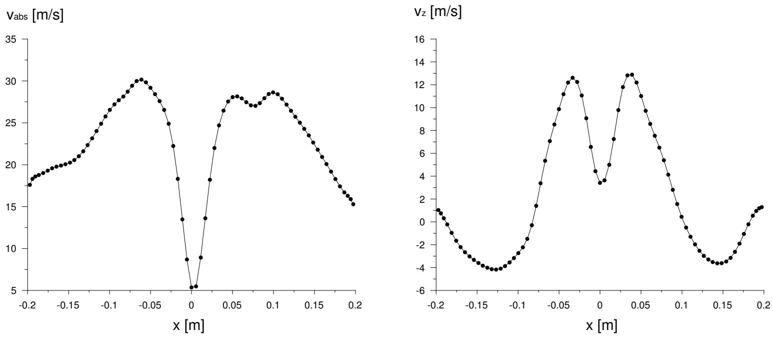


Figure 9: Example for **Class W**. Simulation result for Geometry *Gorton-Hülgerth* De/D=0.375. Number of grid cells: 478 000. Velocity profile 0.125 m below vortex finder in xz-plane. Left: absolute velocity [m/s], right: axial velocity [m/s].

# 3 Measurements

## 3.1 Experimental Equipment

The cylone used in the experiments is derived from the geometry *Fredriksson* by linearily downscaling it by a factor of $f$=0.7.

| | Geometry Fredriksson $f$=0.7 |
|---:|---:|
| D [m] | 0.140 |
| De [m] | 0.056; 0.064; 0.074; 0.084 |
| S [m] | 0.070 |
| s [m] | 0.105 |
| h [m] | 0.210 |
| H [m] | 0.560 |
| a; b; c [m] | 0.070; 0.028; 0.140 |
| B [m] | 0.050 |
| hd; rd [m] | 0.140; 0.094 |
| $\dot{V}$ $[m^3/s]$ | 0.04167 |
| $v_x$ [m/s] | 21.26 |

Table 4: Geometry parameters, volumetric flow rate ($\dot{V}$) and mean flow velocity at entry ($v_x$) for the laboratory cyclone.

It was entirely built of plexiglass™ with interchangable vortex-finders with various diameters and an exchangable dust collector. The equipment used for LDA-Measurements consisted of a LDP 100 (Laser and measuring cell) and a Laservec IFA 600 (Digital burst processor) – both from TSI™. The seeding used was $SiO_2$ with a mean particle diameter of 7 $\mu$m, which was fluidized with pressurised air before it was released into Inlet I1 (see. Fig. 10) to avoid agglomeration effects. The LDA measurements were carried out at a constant air flow rate in the cyclone. Radial profiles of axial velocity were measured 0.16 m below the top cover of the cyclone in the direction indicated in Fig. 10. The pressure drop over the cyclone and the flow rate were determined by a segmental orifice with an area ratio of 0.5 (A1 in Fig. 10) suitable for particle laden flows.

Measurements for two exit conditions at the upper end of the vortex-finder were done (see Fig. 11 and 12):

1. No pipe downstream the vortex-finder V (blowing fan at I1)
2. Bent pipe downstream the vortex finder V (like in Fig. 10 with suction at O1, O2 and O3)

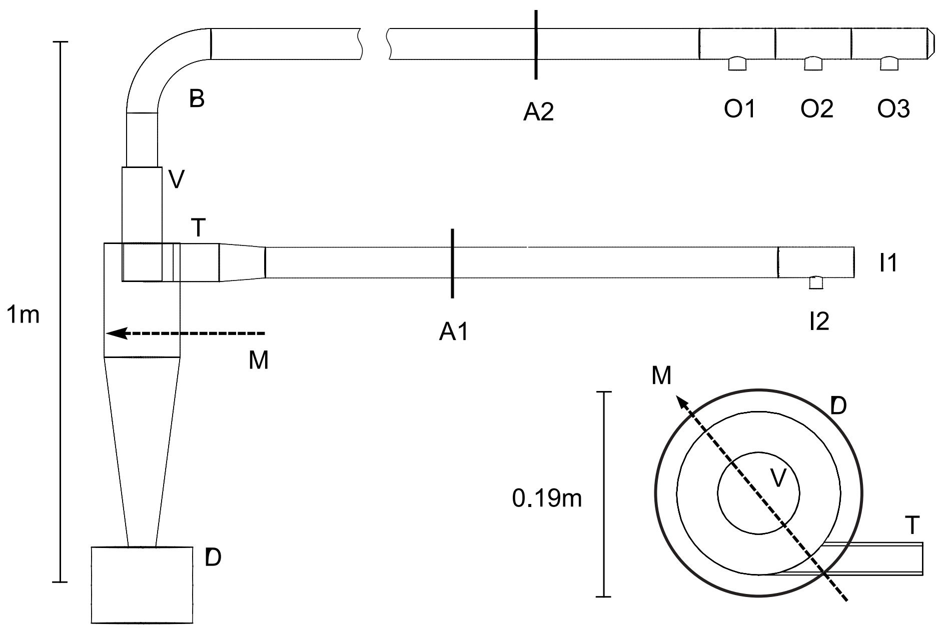


Figure 10: Experimental setup with length scale. *Legend*: A1, A2: Segmental orifices. B: Bent pipe. D: Dust collector. I1, I2: Inlets. M: Measuring direction for LDA. O1, O2, O3: Outlets to fan. T: Tangential inlet. V: Vortex finder. Inner diameter of pipe: d=0.057 m. Distance from *B* to *A2* equals 20 d.

### 3.2 Results

Qualitative agreement between the simulation result and LDA-measurements is found for the laboratory cyclone with De/D=0.5 and no pipe attached downstream the vortex-finder. Measurement and simulation result belong to class W. The same cyclone with a bent pipe downstream the vortex finder displays a very different behaviour with a maximum of axial velocity at the symmetry axis of the cyclone (class V). (see Fig. 11)

Interestingly, the exit condition for geometry De/D=0.4 does not influence the measured profile of z-velocity. The measured profile for this geometry belongs to class W whereas the simulated result belongs to class V. (see Fig. 12)

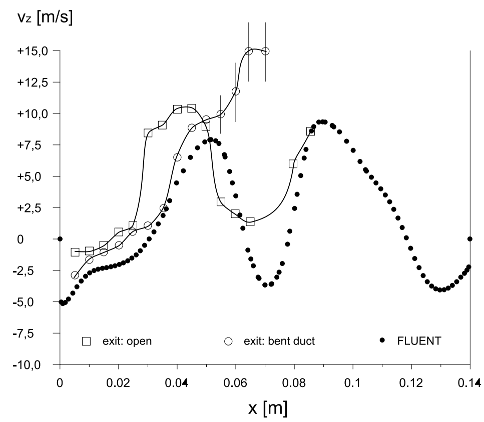


Figure 11: Simulation result and measured axial velocity for laboratory cyclone De/D=0.53. □ : No pipe downstream of vortex-finder, ○ : Bent pipe downstream of vortex finder, • : Simulation result using FLUENT™

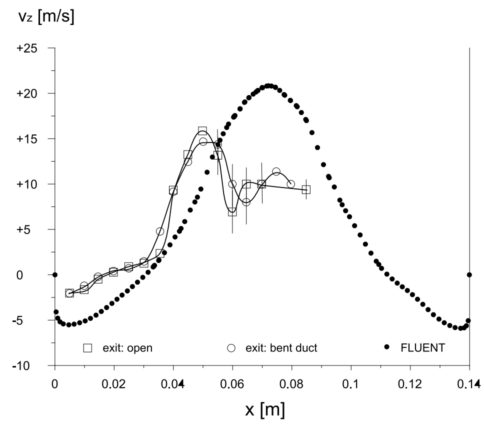


Figure 12: Simulation result and measured axial velocity for laboratory cyclone De/D=0.4. □ : No pipe downstream of vortex-finder, ○ : Bent pipe downstream of vortex finder, • : Simulation result using FLUENT™

# 4 Conclusions

It has been shown that a physically correct simulation result depends on a few important prerequisits: hexahedral grid in main flow regions, RSM and higher order discretisation.

The physical reasons for the development of a V- or W-like profile of axial velocity inside the cyclone are still unknown. Experiments show that the diameter of the vortex-finder does not exclusively influence the development of a certain profile. Downstream exit conditions may play an important role for reversed flow inside the vortex finder and the internal flow structure of the cyclone.

The simulated profile for the laboratory cyclone with De/D=0.5 shows good agreement with the measurements in the region of the vortex core. The simulation result for the geometry with De/D=0.4 would lead to a misclassification of this case. To find the reason for this deviation of the simulation result further investigation is needed.

# 5 Outlook

The influence of exit conditions on the flow structure of simple cyclone designs is not fully understood yet. Further investigations, both simulations and measurements, need to be carried out to generalise the findings. Experiments with other De/D ratios and air flow rates will be carried out and compared with simulation results. Simulations with varying geometry parameters (D, De, H, h, etc.) and various flow rates ($\dot{V}$) will be performed and evaluated by means of chemometric methods to find general dependencies of class membership on dimensionless parameters.

# References


Anh, H. C. (2004). Modellierung der Partikelagglomeration im Rahmen des Euler/Lagrange-Verfahrens und Anwendung zur Berechnung der Staubabscheidung in Zyklonen. PhD-Thesis. Martin-Luther University Halle-Wittenberg.

Boysan, F., Ayers, W., and Swithenbank, J. (1982). Fundamental mathematical modelling approach to cyclone design. *Trans. Inst. Chem. Eng.*, V 60. No.4, p. 222-230.

Fluent (2001). Fluent 6.0 user's guide vol.1.

Frank, T. and Yu, Q. (1999). Experimental and numerical investigation of particle seperation in a symmetrical double cyclone seperator. *Proceedings of the 3rd ASME/JSME Joint Fluids Engineering Conferences.* San Francisco, California, USA.

Fredriksson, C. (1999). Exploratory experimantal and theoretical studies of cyclone gasification of wood powder. PhD-Thesis. Lulea Tekniska Universitet.

Gorton-Hülgerth, A. (1998). Messung und Berechnung der Geschwindigkeitsfelder und Partikelbahnen im Gaszyklon. PhD-Thesis. Technical University Graz.

Griffiths, W. and Boysan, F. (1995). Computational fluid dynamics (CFD) and empirical modelling of the performance of a number of cyclone samplers. *J.Aerosol Science*, 27(2). p. 281-304.

Hoekstra, A., Derksen, J., and Akker, H. V. D. (1999). An experimental and numerical study of turbulent swirling flow in gas cyclones. *Chem.Eng.Science*, 54. p. 2055-2065.

Horvath, A. (2002). Auswirkungen von unterschiedlichen Turbulenzmodellen und Meshes bei der CFD-Simulation der Strömungsverhältnisse in einem Modellzyklon. Technical report, Study-work. TU-Vienna, Inst. of Chem. Eng. – see also http://www.zid.tuwien.ac.at/projekte/2002/02-166-1.pdf.

Kim, J. and Lee, K. (1990). Experimental study of particle collection by small cyclones. *Aerosol Sci. Technol*, 12. p. 1003-1015.

Ma, L., Ingham, D., and Wen, X. (2000). Numerical modelling of the fluid and particle penetration through small sampling cyclones. *J.Aerosol Sci.*, 31. p. 1097-1119.

Noriler, D., Vegini, A., Soares, C., Barros, A., Meier, H., and Mori, M. (2004). A new role for reduction on pressure drop in cyclones using compuational fluid dynamic techniques. *Brazilian Journal of Chemical Engineering*, 21. pp. 93 - 101.

Obermair, S. (2002). Einfluss der Feststoffaustragsgeometrie auf die Abscheidung und den Druckverlust eines Gaszyklons. PhD-Thesis. Technical University Graz.

Peng, W., Boot, P., and Udding, A. (2001). Determining the best modelling assumtions for cyclones and swirl tubes by CFD and LDA. *PARTEC (International Congress for Particle Technology)*.

Slack, M. (2001). QNET-CFD application challenge: Cyclonic seperator. *Fluent Europe ltd.*

Slack, M., Boysan, F., Prasad, R., and Bakker, A. (2000). Advances in cyclone modelling using unstructured grids. *Trans.I.Chem.E.*, 78 Part A. p. 1098-1104.

Solero, G. and Coghe, A. (2002). Experimental fluid dynamic characterization of a cyclone chamber. *Experimental Thermal and Fluid Science*, 27. p. 87-96.

Yoshida, H. (1996). Three-dimensional simulation of air cyclone and particle seperation by a revised-type cyclone. *Physicochemical and Engineering Aspects*, 109. p. 1-12.